

DON BOSCO COLLEGE OF ENGINEERING
FATORDA, MARGAO, GOA – 403 602.

**DEPARTMENT OF ELECTRONICS AND TELECOMMUNICATION
ENGINEERING**

2019 – 2020



**“DEVELOPMENT OF AN EFFECTIVE CLASSIFICATION
TECHNIQUE TO CLASSIFY SETTLEMENTS INTO
VARIOUS LAND COVER FEATURES”**

By

Mr. Sherwin Arnald Colaco

Mr. Shivam Shrivallabh Bale

Mr. Keith Prazeres Pinto

Under the Guidance of

Dr. Varsha Turkar

Head of Department

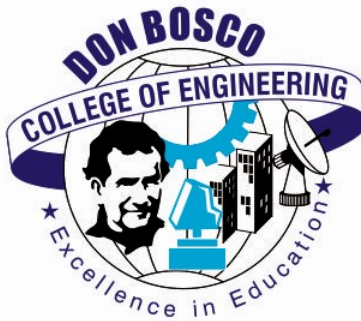
Dr. Shreyas Simu

Assistant Professor

BACHELOR OF ENGINEERING: GOA UNIVERSITY

**DON BOSCO COLLEGE OF ENGINEERING
FATORDA, MARGAO, GOA – 403 602.**

2019 – 2020



CERTIFICATE

This is to certify that this dissertation entitled
**“DEVELOPMENT OF AN EFFECTIVE CLASSIFICATION TECHNIQUE TO
CLASSIFY SETTLEMENTS INTO VARIOUS LAND COVER FEATURES”**
submitted in partial fulfillment of the requirements for Bachelor’s Degree in Electronics
and Telecommunication Engineering of Goa University is the bonafide work of
Mr. Sherwin Arnald Colaco
Mr. Shivam Shrivallabh Bale
Mr. Keith Prazeres Pinto

Dr. Varsha Turkar

INTERNAL GUIDE

Dr. Shreyas Simu

INTERNAL GUIDE

Dr. Varsha Turkar

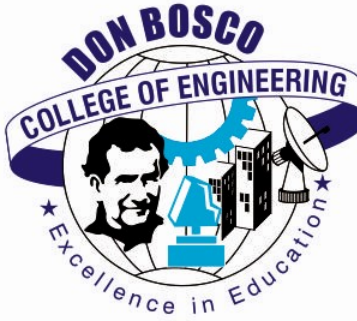
HEAD OF DEPARTMENT

Dr. Neena Panandikar

PRINCIPAL

DON BOSCO COLLEGE OF ENGINEERING
FATORDA, MARGAO, GOA – 403 602.

2019 – 2020



CERTIFICATE

The dissertation entitled,

**DEVELOPMENT OF AN EFFECTIVE CLASSIFICATION
TECHNIQUE TO CLASSIFY SETTLEMENTS INTO VARIOUS LAND
COVER FEATURES**

submitted by

Mr. Sherwin Arnald Colaco
Mr. Shivam Shrivallabh Bale
Mr. Keith Prazeres Pinto

in partial fulfillment of the requirements of the Bachelor's Degree in Electronics and Telecommunication Engineering of Goa University is evaluated and found satisfactory.

DATE: _____

EXAMINER 1: _____

PLACE: _____

EXAMINER 2: _____

ACKNOWLEDGEMENT

It is not possible to complete a project without the assistance and encouragement of other people. In our efforts towards the realization of project work, we have drawn the guidance of many people and we would like to express our heartfelt gratitude to all people who helped in fulfilling the accomplishment of this project. We would like to express our profound gratitude to Our Director, Rev. Fr. Kinley D'Cruz for providing us the necessary infrastructure to carry out our project work easily.

We are highly indebted to our principal, Dr. Neena Panandikar for allowing us to take up this project. We would like to express our deep gratitude to Dr. Varsha Turkar, Head of Department of Electronics and Telecommunication Engineering and our internal project guide and Dr. Shreyas Simu project co-guide for their exemplary guidance, monitoring, unconditional support and constant encouragement throughout that has made our project successful. We also would like to thank them for sparing time and providing necessary information patiently and for their co-operation in preparation of this report. Their constant motivation and inspiration have led to the successful completion of our project targets so far. We would also like to thank all the faculty members of Don Bosco College of Engineering for their critical advice and guidance during various phases of our project.

We also extend our gratitude to ETC Lab Assistants, Technical staff and Librarian for assisting us in bringing together the project and providing resources whenever required by us for our project work. Lastly, we place on records, a deep sense of thankfulness to Almighty, our family and friends for their blessings, inspiration and constant support from the time we ventured into this project till now and those who have helped us directly and indirectly for the accomplishment of the project.

Contents

1 INTRODUCTION	8
1.1 MICROWAVE REMOTE SENSING	8
1.2 SYNTHETIC APERTURE RADAR (SAR)	9
1.3 POLARIMETRIC SAR	9
1.4 RADAR IMAGING SATELLITES	10
2 LITERATURE REVIEW	11
3 RESEARCH GAP	13
4 OBJECTIVES	14
5 METHODOLOGY	15
5.1 PolSAR DATA	15
5.2 SPECKLE REMOVAL	15
5.3 DECOMPOSITION OF IMAGES	16
5.4 CLASSIFICATION	18
6 DATASET	22
7 PROJECT TIMELINE	24
8 RESULTS	25
8.1 TRAINING DATA	25
8.2 CLASSIFIED IMAGES	27
8.3 CONFUSION MATRIX	32
8.3.1 MATRICES FOR DECISION TREE CLASSIFIER MODEL	32
8.3.2 MATRICES FOR ARTIFICIAL NEURAL NETWORK CLASSIFIER MODEL	35
8.3.3 MATRICES FOR RANDOM FOREST CLASSIFIER MODEL	38
8.3.4 PARAMETERS CALCULATED	40
9 COST ANALYSIS	42
9.0.1 CHARACTERISTIC CALCULATIONS	42
9.0.2 COST ESTIMATION	42
10 CONCLUSION	43
11 BIBLIOGRAPHY	44
12 PLAGIARISM CHECK RESULT	45

List of Figures

1	Active & Passive Remote Sensing	8
2	Microwave Frequency Bands	9
3	Synthetic Aperature Radar	9
4	methodology	15
5	PolSAR image affected with speckle noise	15
6	Back Scattering	17
7	Artificial Neural Network Layout	19
8	Random forest generated model	20
9	Binary decision tree	21
10	San Francisco	22
11	Pauli RGB Image	23
12	Project timeline	24
13	seven component training data	25
14	Four Component training data	26
15	Three component training data	26
16	Decision tree classifier image:using three component data	27
17	Decision tree classifier image:using four component data	28
18	Decision tree classifier image:using seven component data	28
19	Random Forest classifier image:using three component data	29
20	Random Forest classifier image:using four component data	29
21	Random Forest classifier image:using seven component data	30
22	ANN classifier image:using three component data	30
23	ANN classifier image:using four component data	31
24	ANN classifier image:using seven component data	31
25	Confusion matrix:Decision tree classifier model trained using 3 component data	32
26	Confusion matrix:Decision tree classifier model trained using 4 component data	33
27	Confusion matrix:Decision tree classifier model trained using 7 component data	34
28	Confusion matrix:ANN classifier model trained using 3 component data	35
29	Confusion matrix:ANN classifier model trained using 4 component data	36
30	Confusion matrix:ANN classifier model trained using 7 component data	37
31	Confusion matrix:Random Forest classifier model trained using 3 component data	38
32	Confusion matrix:Random Forest classifier model trained using 4 component data	39
33	Confusion matrix:Random Forest classifier model trained using 7 component data	40
34	Plagiarism check result	45

Abstract

Although India is one of the less urbanized countries of the world with only 27.78% of the population living in urban agglomerations, the country is facing a serious crisis of Urban growth at the present time. Urbanization has been an instrument of economic, social and political progress but it has also led to serious socio-economic problems. The sheer magnitude of urban population, haphazard and unplanned growth of urban areas and a desperate lack of infrastructure are the main causes of such a situation.

Effective Urban Planning is a simple but powerful solution in order to ensure that such problems do not persist in the years to follow or are at least reduced to an acceptable minimum. Settlement planning requires hours of deep analytic study on existing settlement information as well as information on surrounding areas in a particular region. In order to obtain this information, officials will need to survey large amounts of data with a minimum amount of on-field work.

Remote sensing uses satellites to capture images and can survey large areas at a time in a matter of seconds which would normally take months of manual surveying for a field professional. Since satellite image datasets are readily available on the internet today for all regions, the use of remote sensing provides the best possible approach which satisfies a majority of the objective criteria required for urban classification.

In this project we aim to develop an effective classification technique to classify microwave images and categorize the identified settlements into various landcover features such as slums, residential areas, open spaces, forest, lakes, etc. which will help in the urban planning process.

1 INTRODUCTION

Remote sensing is the process of acquiring information about the earth's surface without coming in contact with it. This is done by emitting energy and recording the reflected energy back which is further processed and analyzed to obtain information. Remote sensing is further subdivided into two categories

1. Active Remote sensing: The antenna itself emits radiation that is then received to form an image at the receiver.
2. Passive Remote sensing: Such systems make use of the energy radiated by the sun for imaging purposes they do not emit radiation of their own and hence depend on the sun's energy for their functioning.

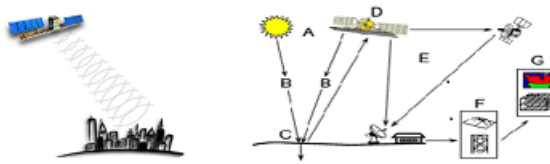


Figure 1: Active & Passive Remote Sensing
(source:<https://staff.aub.edu.lb/~webeco/rs%20lectures.htm>)

1.1 MICROWAVE REMOTE SENSING

Microwave Sensing includes active as well as passive forms of remote sensing systems that measure the energy that is naturally existing i.e. sunlight are called passive remote sensors, they can only be used to detect energy when energy is naturally occurring. Active sensors, on the other hand, illuminate the required object using an independent energy source. Radiation is emitted by the active sensor which then falls on the target that is under investigation and the reflected radiation is measured by the sensor. The advantage of using active sensors is that the measurements can be obtained anytime regardless of the time of day or season. Microwaves have a longer wavelength compared to Visible and infrared waves in the electromagnetic spectrum thus microwaves have special properties that are important for remote sensing. Longer wavelength microwave radiations can penetrate through cloud cover, haze, dust, and the heaviest rainfall as microwave wavelengths are not susceptible to atmospheric scattering which is the main problem when dealing with shorter optical wavelengths. Thus, microwave energy can be detected under almost all weather and environmental conditions so that informative data can be collected at any time. The microwave region of the spectrum is initially quite large as compared to visible and infrared and there are several wavelength ranges or bands that microwaves are commonly divided into

- Ka, K and Ku band: very early airborne radar systems but uncommon today.
- X- Band: Used extensively on airborne systems for military purposes and terrain mapping
- C- Band: Commonly used in airborne research systems
- S-Band: used onboard the Russian ALMAZ satellite
- P-Band: contains the longest wavelength and is used on NASA experimental airborne research systems

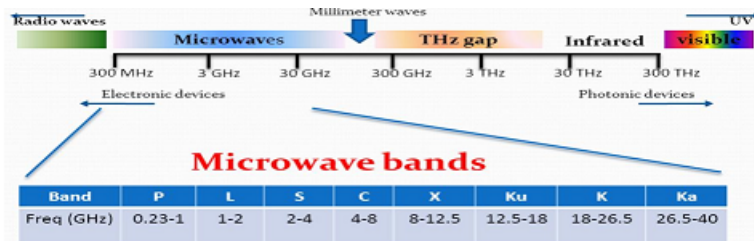


Figure 2: Microwave Frequency Bands
 (source: <https://www.pgc.umn.edu/guides/commercial-imagery/intro-satellite-imagery/>)

1.2 SYNTHETIC APERTURE RADAR (SAR)

SAR also known as Synthetic Aperture Radar is the method of achieving a uniform, fine azimuth resolution across the entire image swath. The use of SAR for remote sensing is particularly suited for tropical countries. Since SAR is an active sensor, which provides its own source of illumination, it can, therefore, operate day or night; able to illuminate with variable look angle and can select wide area coverage. In addition, the topography change can be derived from the phase difference between measurement using radar interferometry.

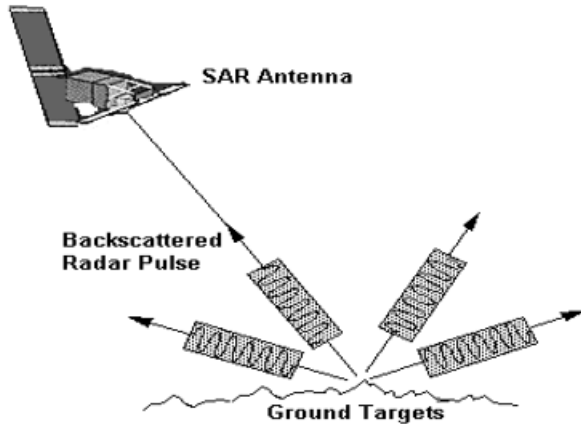


Figure 3: Synthetic Aperture Radar
 (source:<https://crisp.nus.edu.sg/~research/tutorial/mw.htm>)

1.3 POLARIMETRIC SAR

Polarimetric SAR or PolSAR systems enhance the capabilities of any basic radar systems by allowing the sensors to transmit and receive in multiple polarizations, by utilizing different polarizations we can identify unique and distinct features of the target. Some features that can be observed in one polarization cannot be observed in another polarization. A target's characteristic is defined more clearly by combining all polarization modes. In basic

terms, a radar system can transmit and receive either a Horizontal (H) Or a Vertical (V) polarization of a radio wave. Polarimetric SAR can be performed by either transmitting horizontal or vertical polarizations or by receiving horizontal or vertical polarization, or both.

There can be 4 combinations of transmitting and receiving polarizations :

- HH: - For horizontal transmit and horizontal receive.
- VV: - For vertical transmit and vertical receive.
- HV: - For horizontal transmit and vertical receive.
- VH: - For vertical transmit and horizontal receive.

The first two polarization (HH & VV) combinations are referred to as “like polarized”. The last two polarization (HV & VH) combinations are referred to as “cross-polarized”.

1.4 RADAR IMAGING SATELLITES

Radar is developed to detect the presence of a target and to find the distance of a target from the radar by using radio waves.

Radar transmits short bursts or pulses of microwave signals in the direction of the object and records the strength of the received signal along with the time required to return it back. Radar antennas are attached to aircrafts known as Airborne radars or satellites known as spaceborne radars in order to produce images of earth known as an imaging radar.

The look angle and the swath coverage are affected by altitude variations of the radar. Some operational spaceborne SAR systems are mentioned below

- ENVISAT-1 launched in March 2002 and uses frequencies lying in the C-band of microwaves for imaging
- RADARSAT-2 launched in December 2007 uses frequencies lying in the C-band of microwaves for imaging
- ALOS-1 launched in January 2006 uses frequencies lying in the L-band of microwaves for imaging
- ALOS-2 will continue the L-band SAR observations of the ALOS PALSAR (Phased Array L-band Synthetic Aperture Radar) and will expand data utilization by enhancing its performance.
- TerraSAR-X launched in June 2007 uses frequencies lying in the X-band of microwaves for imaging
- RISAT-1 launched in April 2012 uses frequencies lying in the C-band of microwaves for imaging
- UAVSAR- (Unmanned Aerial Vehicle Synthetic Aperture Radar) uses frequencies lying in the L-band of microwaves for imaging
- AIRSAR-(Airborne Synthetic Aperture RADAR) uses frequencies lying in the L-band C-band as well as P-band of microwaves for imaging

An AIRSAR dataset of the San Francisco Bay region was used for this project since datasets of this sensor are freely available over the internet.

2 LITERATURE REVIEW

Urban classification like the land-cover and land-use classification is one of the most important applications of PolSAR. Many algorithms have been developed for supervised and unsupervised Urban classification. In supervised classification, training sets for each class are selected, based on ground truth. For each pixel, the PolSAR gives information in three real and three complex parameters. When ground truth maps are not available, it makes the selection of training sets difficult. Unsupervised classification classifies the image automatically by finding clusters based on a certain criterion (similarity and dissimilarity). However, the final class recognition is done manually. PolSAR images are affected by noise called speckle. Noise appears in PolSAR images due to the coherent interference of waves reflected from many elementary scatters. Speckle in PolSAR images affects the image interpretation and reduces the classification accuracy. To avoid this various speckle filters can be used.

The fundamental concepts of Microwave Remote Sensing explains how images are acquired from satellites and various satellites that are used in the process. The various properties of the microwaves and its applications are covered in [2]. Pre-processing techniques, image enhancement, transformation and classification of digital images are also explained in brief.

[2] proposes the use of Random Forests as classification method for building detection, which is able to deal with a broad variety of different features and are designed to include contextual knowledge as well. Random Forests can be designed to exploit contextual knowledge, and therefore surpass pixel-based classification methods. Random Forests grow several trees, each of them considered as weak classifier, and combine their output to obtain a classifier, whose performance is more accurate and robust than that of every single tree alone. During the training of each tree, the training image is divided into several overlapping, randomly distributed patches. Therefore, each training sample has a dimensionality of $S \times S \times F$, where S is the patch size and F the number of used features. Each internal node projects this high-dimensional data point p to a single dimension by the usage of a specific projection function. All the parameters of the projection including the type of projection are chosen randomly. Only one feature is involved in one projection. The local context of a pixel is used. It is assumed, that objects of the same class should consist of similar structures, which will lead to similar projections. Images are structured data and contain context information. This kind of information was firstly exploited by the usage of specific features like texture, which are based on spatial neighbourhoods. Secondly, it was used during the induction of each tree, since each projection is based on the local neighbourhood of a pixel. Class estimation of a specific pixel often contains useful information about the probable class estimations of its neighbours. Therefore, in each leaf node n not only the probability for the patch's central pixel is stored, but the spatial probability distribution of the whole patch. Since the layover effect causes the image of high buildings to merge with those of surrounding buildings, not all image areas of single buildings are clearly distinguishable. However, if there is enough distance then single buildings are clearly identifiable.

The researchers in [4] proposed a method, where Genetic Algorithm (GAs) and Support Vector Machines (SVMs) or Multi-Layer Perceptron neural networks were used on the decomposed results that maximized classification accuracy. The averaged classification accuracy of the proposed method reached up to 95%.

[7] processed polarimetric SAR data from ALOS PALSAR, ENVISAT ASAR and SIR-C for classification of wet and arid lands. Their results from Mumbai data show that ALOS HH & HV data is better than ASAR HH&VV for the classification of wet lands. Using SIR-C fully polarimetric data water logged areas including ponds and lakes identified.

Multi-frequency and multi-polarized data can be classified using MDC, MLC, ANN, SVM and DTC as mention in [8]. The researchers explained how classification accuracy increases after combining different polarizations of SIR-C L- and C-band. It was found that the classification accuracy further improves after applying Enhanced Lee

Filter. Similarly, RADARSAT-2 C-band, ALOS PALSAR L-band and TerraSAR X-band data over Mumbai were classified individually and in combination. The land cover classification capabilities of fully versus partially and hybrid polarimetric SAR data for L- and C-band were studied. An effective technique for classification of urban areas which are not orthogonal to the radar Line of Sight is by using polarization orientation compensation (POC) and Circular Correlation Coefficient (CCC). The proposed method increases the classification accuracy by 40%.

[11] proposed a technique to find indices of polarimetric correlation coefficient in linear and circular polarization bases to extract useful features from polarimetric SAR data. These indices were selected by the applicability of the polarimetric analysis based on the polarimetric scattering model and the property of azimuthal symmetry. This technique was applied to Pi-SAR/X-SAR data. This technique shows its capability to discriminate between vegetation area and the urban area.

[4] proposed a novel semi-supervised Dimensionality Reduction(DR) algorithm SNC for PolSAR feature extraction and terrain classification. The content explains how a low-dimensional subspace is learned from the original high-dimensional feature space of PolSAR data by a designed objective function. The spatial groups are constructed from the adjacent pixels in the image domain and used as the basic unit during DR, which weakens the influences of the speckle noise. Classification accuracies on a variety of PolSAR data obtained prove that the separability of the data is greatly enhanced with the SNC algorithm. The SNC performs well not only on the homogeneous terrains but also the heterogeneous terrains such as urban from different PolSAR systems. The only drawback of the proposed algorithm is that the algorithm has difficulty in distinguishing pixels on the boundaries of classes.

[9] attempts to assign one such physical scattering model to the real part of T23 ($\text{Re}\{\text{T23}\}$) and develop a new scattering power decomposition model, called as the seven component scattering decomposition (7SD). The physical scattering model for $\text{Re}\{\text{T23}\}$ is derived from a particular configuration of dipoles (referred to as “mixed dipole” configuration), which gives rise to compound scattering. In earlier models the problem pertaining to $\text{Re}\{\text{T23}\}$ was not realized because the $[\text{T}]$ matrix was compensated for the orientation of the target about the radar line of sight (LoS). This compensation reduced $\text{Re}\{\text{T23}\}$ to zero. The seven components that were described by G.Singh are Ps , Pd , Pv , Ph , Pod , Pcd , and Pmd . $[\text{T}]_s$, $[\text{T}]_d$, $[\text{T}]_v$, $[\text{T}]_h$, $[\text{T}]_{od}$, $[\text{T}]_{cd}$, and $[\text{T}]_{md}$ are the scattering submatrices that were acquired by surface scattering, double-bounce scattering, volume scattering, helix scattering, oriented dipole scattering, compound dipole scattering (oriented quarter-wave reflectors scattering), and mixed dipole scattering, respectively. The highlight of this model was that it worked on the original coherency matrix without any transformation. The compound scattering derived from the mixed dipole configuration finds its application in identifying man-made structures and species of vegetation where the branches have the mixed dipole or combination of dihedral configurations.

This paper [8] attempts to assign one such physical scattering model to the real part of T23 ($\text{Re}\{\text{T23}\}$) and develop a new scattering power decomposition model, called as the sevencomponent scattering decomposition (7SD). The 7 components that are obtained are as follows.

Ps , Pd , Pv , Ph , Pod , Pcd , and Pmd are the scattering powers to be determined. $[\text{T}]_s$, $[\text{T}]_d$, $[\text{T}]_v$, $[\text{T}]_h$, $[\text{T}]_{od}$, $[\text{T}]_{cd}$, and $[\text{T}]_{md}$ are the scattering submatrices that are acquired by surface scattering, double-bounce scattering, volume scattering, helix scattering, oriented dipole scattering, compound dipole scattering (oriented quarter-wave reflectors scattering), and mixed dipole scattering, respectively. The highlight of the new proposed model is that it works on the original coherency matrix without any transformation. Since the model accounts for $\text{Re}\{\text{T23}\}$, it retains $\text{Re}\{\text{T23}\}$. The compound scattering derived from the mixed dipole configuration finds its application in identifying man-made structures and species of vegetation where the branches have the mixed dipole or combination of dihedral configurations.

3 RESEARCH GAP

The previous work in this field includes the use of microwave radar satellite images for a wide range of applications. These include classification of images based on various landforms such as water, settlements and forests. Classification has also been used to categorize regions depending on vegetation characteristics which have been used to identify and differentiate between various crop species. Previous applications, however, do not include the use of satellite image classification to distinguish between various land cover features. The proposed system will classify satellite images based on various land cover features such as slums, towns, cities etc. These images can be used by government officials to facilitate effective urban planning.

4 OBJECTIVES

The main objective of this project is to create a system that will classify satellite images of the selected region in order to provide government officials with sufficient information on settlements in the area in order to aid them in urban planning process.

The design process of such a system will include the following steps

1. Classify the settlement using conventional (existing) filters using various windows sizes.
2. Classify the settlements using decomposed images.
3. Classify the settlement using coherency or covariance matrix,
4. Compare the results of step (2) and step (3)
5. Select the method with best results of the two for the urban classifier.

5 METHODOLOGY

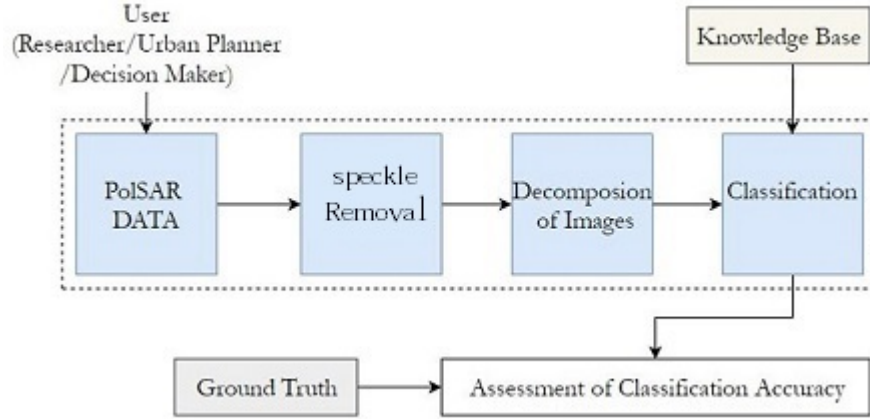


Figure 4: methodology

5.1 PolSAR DATA

Various datasets are available online. These datasets span over different frequency bands such as L-band C-band, and P-band, etc. Each band provides varying depths of information of the same ROI due to their varying wavelengths. The focus of this project is to use satellite images within the L-band frequency range to classify various land cover features. For our requirements sample datasets were collected from different sources over the internet. The city of San Francisco (AirSAR dataset) was selected for this purpose.

5.2 SPECKLE REMOVAL

Speckle noise is a granular interference that inherently exists in and degrades the quality of the active synthetic aperture radar (SAR) image.

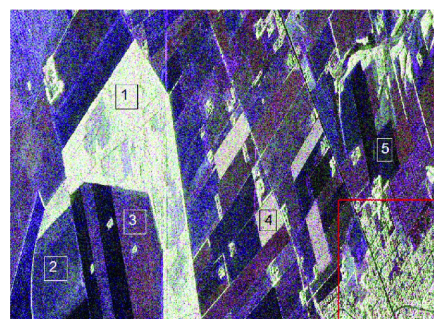


Figure 5: PolSAR image affected with speckle noise

(source:www.researchgate.net%2Ffigure%2FEMISAR-L-band-PoSAR-image-from-Foulum-in-Denmark-Five-homogeneous)

5.3 DECOMPOSITION OF IMAGES

Polarimetric Synthetic Aperture Radar (PolSAR) is sensitive to the geometric structure, orientation and physical characteristics of scattering targets. Polarimetric Target Decomposition (PTD) is a useful tool to identify and separate scattering mechanisms. The objective of Target decomposition (TD) theory is to express the average scattering mechanism as the sum of independent elements to associate a physical mechanism with each component. There are two types of TD. One is Coherent (CTD) and other is Incoherent (ICTD).

Coherent Decomposition

CTD was developed to characterize completely polarized scattered waves for which fully polarimetric information is contained in the scattering matrix. The CTD can be used only to study coherent targets also known as point or pure targets. Manmade objects are the example of pure targets. Pauli, Krogager, Cameron are Coherent type of decomposition.

In-coherent Decomposition

ICTD was developed to characterize distributed scatterers. Freeman, Van Zyl and Yamaguchi are different types of ICTD. Freeman and Van Zyl has three types of scattering mechanisms namely volume, double bounce and surface or single bounce. Yamaguchi 4- component has one additional scattering mechanism that is helix. Helix scattering often appears in complex urban areas where it disappears in almost all natural distributed scenarios.

One of the most used PTD methods is the three-component decomposition method, which decomposes PolSAR data into three categories: surface or single-bounce, double-bounce, and volume-bounce. This approach is best when either double bounce contribution or surface contribution is close to zero. In real cases, especially in double-bounce and single-bounce contribution, speckle will be introduced due to artificial settings (issues related to the satellite). Another problem of the three-component decomposition method is that the volume scattering power is usually overestimated in oriented urban areas. Therefore [7] added a fourth helix component to their decomposition to account for the disadvantages of the 3 component decomposition.

Polarimetric decomposition approaches provide a measure of the relative contributions of backscatter from different scattering mechanisms and hence, the selection of proper decomposition methods plays a vital role in the classification of natural distributed targets. Over the years a number of newer decomposition models have been introduced by scientists like Gulab Singh [ref no.] that are more efficient and provide more information on scattering components. Different Models of Decomposition that were proposed:

- FDD [6]: The pioneering work of all model-based scattering power decomposition, the FDD fits three simple scattering mechanisms to explain the dominant scattering mechanisms of surface, double-bounce, and volume, assuming the condition of reflection symmetry for naturally occurring targets.
- Yamaguchi Four-Component Original (Y4O) [7]: For targets that do not obey the reflection symmetry condition, the Y4O model explains the helix scattering.
- Four-Component Scattering Power Decomposition With Extended Volume Scattering Model (S4R) : In an attempt to improve FDD and Y4O a disorientation, or desyng operation is performed on $[T]$ using the rotation matrix $[R(\theta)]$. This rotation operation reduces the number of independent parameters of $[T]$ from nine to eight, thus increasing the percentage of information extracted in Y4R [12]. Similar to the Y4R model, S4R incorporates the rotation of the coherency matrix, making $\text{Re}\{T_{23}\} = 0$ and minimizing the depolarized term from T_{33} . However, it discriminates volume scattering coming from the vegetation and oriented-dihedral structures by implementing the extended volume scattering model for dihedral to improve the discrimination

of oriented-urban areas from vegetation. There still exists the issue of identifying scattering from structures in highly oriented urban areas that cannot be solved by S4R model alone. The solution to this problem is addressed in the latest six-component scattering power decomposition that accounts for two new scattering mechanisms.

- Six-Component Scattering Matrix Power Decomposition (6SD) : 6SD model addresses the above-mentioned problem by introducing two new physical scattering models of oriented-dipoles (od) and compound-dipole (cd) structures for $\text{Re}\{\mathbf{T}_{13}\}$ and $\text{Im}\{\mathbf{T}_{13}\}$ elements, respectively. Details of the submatrices along with the implementation of the six-component scattering powers from the rotated coherency matrix are given in .
- Six-Component Scattering Matrix Power Decomposition (6SD) : $P_s, P_d, P_v, P_h, P_{od}, P_{cd}$, and P_{md} are the scattering powers to be determined. $[\mathbf{T}]_s, [\mathbf{T}]_d, [\mathbf{T}]_v, [\mathbf{T}]_h, [\mathbf{T}]_{od}, [\mathbf{T}]_{cd}$, and $[\mathbf{T}]_{md}$ are the scattering submatrices that are acquired by surface scattering, double-bounce scattering, volume scattering, helix scattering, oriented dipole scattering, compound dipole scattering (oriented quarter-wave reflectors scattering), and mixed dipole scattering, respectively.

For the purpose of this project the following decompositions models were used for classification purposes and their results were compared to check classification efficiency.

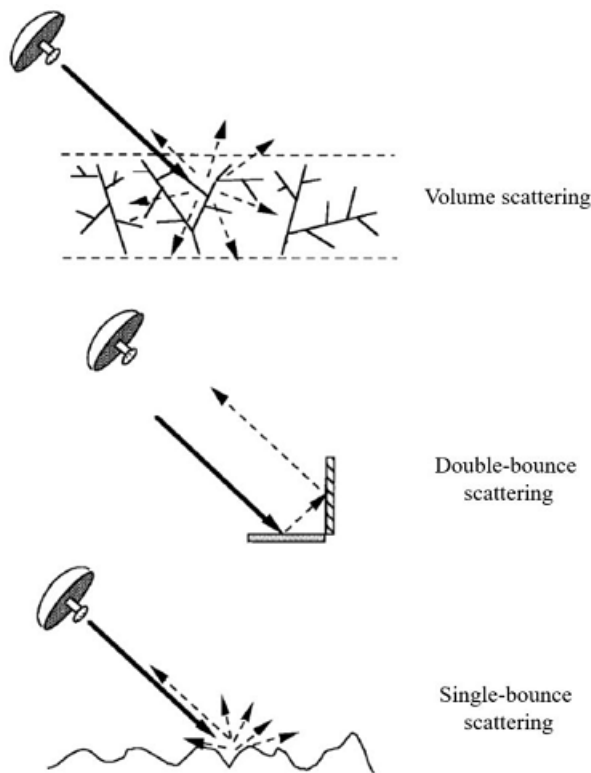


Figure 6: Back Scattering
 (source:[https://www.semanticscholar.org/paper/Polarimetric-Synthetic-Aperture-Radar-\(SAR\)-for-and-Choe/82fc573e489453cca60f502818edc5d2e0ae5296](https://www.semanticscholar.org/paper/Polarimetric-Synthetic-Aperture-Radar-(SAR)-for-and-Choe/82fc573e489453cca60f502818edc5d2e0ae5296))

5.4 CLASSIFICATION

Classification is the task of assigning a set of given data elements to a given set of labels or classes such that the cost of assigning the data element to a class is minimum. Classification of polarimetric SAR images has become a very important topic after the availability of Polarimetric SAR images through ENVISAT ASAR, ALOS PALSAR, SIR-C and Radarsat2.

Urban classification involves classifying decomposed images into various land cover features such as slums, residential areas, open spaces, forest, lakes, etc.

This can be achieved using two broad categories of classifiers:

PARAMETRIC CLASSIFIERS

Parametric classifiers make use of algorithms that simplify the function to a known form and are called parametric machine learning algorithms.

It proposes a learning model that summarizes data with a set of parameters of fixed size (independent of the number of training examples). parametric classifiers have fixed number of parameters irrespective of the amount of data to be classified.

Some more examples of parametric machine learning algorithms include:

- Logistic Regression
- Linear Discriminant Analysis
- Perceptron
- Naive Bayes
- Simple Neural Networks

Benefits of Parametric Machine Learning Algorithms:

- Simpler: These methods are easier to understand and interpret results.
- Speed: Parametric models are very fast to learn from data.
- Less Data: They do not require as much training data and can work well even if the fit to the data is not perfect.

NON-PARAMETRIC CLASSIFIERS

Algorithms that do not make strong assumptions about the form of the mapping function are called nonparametric machine learning algorithms. Nonparametric methods are used when there is a lot of data and no prior knowledge of the desired outcome is available.

Some more examples of popular nonparametric machine learning algorithms are:

- k-Nearest Neighbors
- Decision Trees like CART C4.5
- Support Vector Machines

Benefits of Nonparametric Machine Learning Algorithms:

- Flexibility: Capable of fitting a large number of functional forms.
- Power: No assumptions (or weak assumptions) about the underlying function.
- Performance: Can result in higher performance models for prediction.

ARTIFICIAL NEURAL NETWORKS

Artificial Neural Networks or ANN is an information processing paradigm that is inspired by the way the biological nervous system such as brain processes information. It is composed of large number of highly interconnected processing elements called neurons that work in unison to solve a specific problem. Learning in a neural network is closely related to how we learn in our regular lives and activities. Neural networks require a trainer in order to describe what should have been produced as a response to a given input. Based on the difference between the actual value and the predicted value, an error value is computed and sent back to the system. For each layer of the network, the error value is analyzed and used to adjust the threshold and weights for the next input. The main aim is to minimize the error. The lower the error value, the closer the actual value to the predicted value. In this way, the error keeps becoming marginally lesser in each run as the network learns how to analyze values. In order to simulate a neural network in MATLAB for the purpose of this project, an inbuilt function newff was used. newff in MATLAB creates a feedforward backpropagation network by taking training samples and expected results from the user.

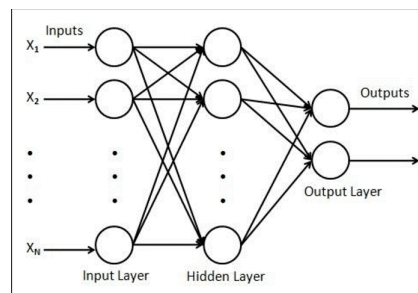


Figure 7: Artificial Neural Network Layout

(source:https://www.researchgate.net/figure/Feedforward-backpropagation-neural-network-topology_fig4_266201206)

The newff function, newff(PR,[S1 S2...SNl],{TF1 TF2...TFNl},BTF,BLF,PF) takes the following parameters

- PR -- R x 2 matrix of min and max values for R input elements
- Si -- Size of ith layer, for Nl layers
- TFi -- Transfer function of ith layer, default = 'tansig'
- BTF -- Backpropagation network training function, default = 'traingdx'
- BLF -- Backpropagation weight/bias learning function, default = 'learngdm'
- PF -- Performance function, default = 'mse'

and returns an N layer feed-forward backprop network.

During implementation of the newff function the number of hidden layers was set to 20. All other parameters were set to their default values.

RANDOM FOREST

Random forest, like its name implies, consists of a large number of individual decision trees that operate as a group. Each tree in the forest is formed by taking different unique features or combinations of features of training samples at random and creating levels of decision nodes to form trees. Due to the randomness of the training sample selection process a number of trees can be obtained.

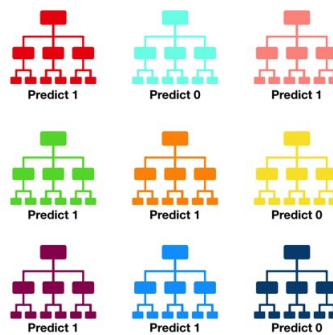


Figure 8: Random forest generated model
(source:<https://www.mathworks.com/help/stats/random-forest.html>)

Each individual tree in the random forest spits out a class prediction and the class with the most votes becomes the Random Forest model's prediction. Hence it can be summarized that the random forest classifier consists of a combination of tree classifiers where each classifier is generated using a random vector sampled independently from the input vector, and each tree casts a unit vote for the most popular class to classify an input vector. For the purpose of this project which was simulated in MATLAB, The Treebagger function was used. Treebagger is an inbuilt function available in MATLAB which in default mode simulates the Breiman's Random forest model also known as Breiman's Bagging model. The predict function, another inbuilt function available in MATLAB was then used to classify test samples by running them through the generated RF model that was obtained in the previous process.

The treebagger function contains two methods that it can perform. These include classification and regression. Other parameters include:

- 'NumPrint' Number of training cycles (grown trees) after which TreeBagger displays a diagnostic message showing training progress. Default value is no diagnostic messages.
- 'MinLeafSize' Minimum number of observations per tree leaf. Default value for it is 1 for classification and 5 for regression.

During implementation of the function treebagger the number of trees to be generated were set to 50 and the mode was set to classification. All other values were set to their default values.

DECISION TREES

A decision tree is a decision support tool that uses a tree-like graph or model of decisions and their possible consequences. Decision trees also referred to as classification trees and regression trees is a predictive model that

maps from observations about an item. To predict a response, The data is continuously split according to a certain parameter. The tree can be explained by two entities, namely decision nodes and leaves. The leaves are the decisions or final outcomes. And the decision nodes are where the data is split. Classification trees give responses that are nominal, such as 'true' or 'false'. Regression trees give numeric responses. Each step in a prediction involves checking the value of one predictor. For example, here is a simple classification tree:

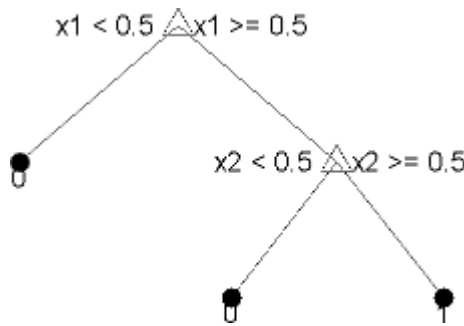


Figure 9: Binary decision tree

(source:<https://www.mathworks.com/help/stats/decision-trees.html>)

This tree predicts classifications based on two predictors, x_1 and x_2 . To predict, start at the top node, represented by a triangle (Δ). The first decision is whether x_1 is smaller than 0.5. If so, follow the left branch, and see that the tree classifies the data as type 0. If, however, x_1 exceeds 0.5, then follow the right branch to the lower-right triangle node. Here the tree asks if x_2 is smaller than 0.5. If so, then follow the left branch to see that the tree classifies the data as type 0. If not, then follow the right branch to see that the tree classifies the data as type 1.

In MATLAB, fitctree which is an inbuilt function was used to implement decision tree since the function returns a binary classification decision tree based on the input variables given by the user. The predict function, was then used to classify test samples by running them through the generated Decision tree model that was obtained in the previous process.

The default values of the tree depth controllers for growing classification trees are:

- $n - 1$ for MaxNumSplits where n is the training sample size
- 1 for MinLeafSize.
- 10 for MinParentSize
- These default values tend to grow deep trees for large training sample sizes

During implementation all variables were set to their default values.

6 DATASET

The focus of this project is to use satellite images within the L-band frequency range to classify various land cover features. For our requirements sample datasets were collected from different sources over the internet. The city of San Francisco was selected for this purpose since AIRSAR datasets for this city were freely available.

San Francisco is extremely dense; it is a very well-planned city with very minimal area available for expansion.

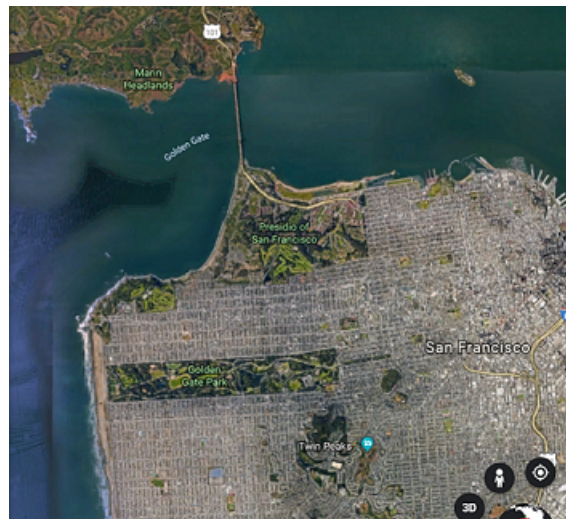


Figure 10: San Francisco
(Source:https://www.google.com/intl/en_in/earth/)

PAULI RGB IMAGES

Fig.9 shows the Pauli RGB image obtained. The image represents single bounce double bounce and volume bounce information using different colours. Single bounce is represented with blue colour, double bounce is represented using red and volume bounce information is represented using green. This image can then be used to further classify the image.

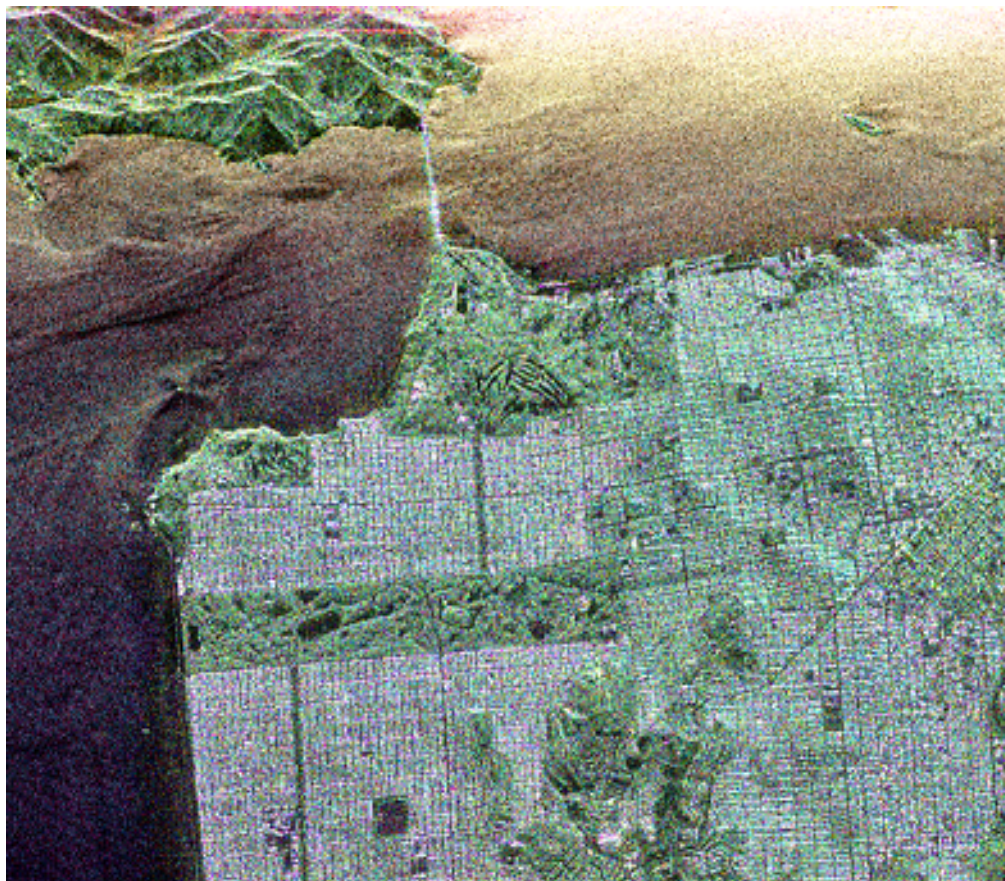


Figure 11: Pauli RGB Image

7 PROJECT TIMELINE



Figure 12: Project timeline

Due to the inconveniences caused due to the sudden COVID-19 lockdown, progress of the project was halted beyond March 16 2020.

8 RESULTS

POLSAR PRO V.4.2 was used to implement image processing , three component and four component decomposition and was also used to classify the available AirSAR dataset in order to study how an image classifier works. Image processing techniques were applied on the images. Pauli RGB image was obtained by sampling available dataset, out of the various filters available Lee Filter was applied to the image to filter out noise component.

After studying how a classifier works a MATLAB code was later developed to use ANN, decision tree and Random forest classifiers on the existing dataset to classify the image.

8.1 TRAINING DATA

During execution of the MATLAB code the user was prompted to select training areas with the pauli RGB image acting as a reference. Data from areas selected by the user in the corresponding three component, seven component and four component datasets were extracted and 3 different training datasets each containing three component, four component and seven component data respectively were obtained. The obtained datasets were then used to create nine different models to classify the image. These include 3 decision tree models, 3 random forest models and 3 Artificial neural network models for three component, four component and seven component data respectively.

	1	2	3	4	5	6	7
1	0.0801	0.0399	0.1460	0.0039	0.0336	0.0173	0
2	0	0	0	0	0	0.3390	0.0655
3	0.0293	0.0568	0.0048	0	0.0598	0	0
4	0.0277	0.0101	0.0267	0.0203	0.0277	0	0
5	0	0	0	0	0	0.0852	0.0452
6	0	0	0	0	0	0	0.0665
7	0	0	0	0	0	0.0271	0.0442
8	0.0133	0.0323	0.0045	0	0.0237	0	0
9	0	0	0	0	0	0.0821	0.0254
10	0.0069	0.0110	0.0182	0.0101	0.0073	0.0087	0.0115
11	0.0120	9.5911e-04	0.0417	0.0191	0.0178	0	0
12	0.0270	0.0071	0.0384	0.0080	4.4610e-04	0.0169	0

Figure 13: seven component training data

The screenshot shows a MATLAB interface with three tabs at the top: 'datasheet_gulab7', 'datasheet_yama3', and 'datasheet_yam'. The active tab is 'datasheet_gulab7', which is described as a 169138x4 double matrix. The table itself has five columns labeled 1, 2, 3, 4, and an unlabeled fifth column. The first few rows of data are:

	1	2	3	4	
1	0.0298	0.1644	0.0654	0.0399	
2	0.3253	0.0342	0.0362	0.0156	
3	0	0	0.0938	0.0568	
4	0.0032	0.0782	0.0259	0.0101	
5	0.0959	0.0062	0.0226	0	
6	0	0	0.0534	0.0053	
7	0.0363	0.0071	0.0221	0	
8	0.0414	0.0062	0.0207	0	
9	0.0667	0.0162	0.0244	5.4001e-04	
10	0	0	0.0626	0.0110	
11	0	0.0532	0.0374	9.5911e-04	
12	0.0045	0.0461	0.0347	0.0071	

Figure 14: Four Component training data

The screenshot shows a MATLAB interface with three tabs at the top: 'datasheet_gulab7', 'datasheet_yama3', and 'datasheet_yam'. The active tab is 'datasheet_gulab7', which is described as a 169138x3 double matrix. The table itself has four columns labeled 1, 2, 3, and 4. The first few rows of data are:

	1	2	3	4
1	0.0312	1.5615e-05	0.0025	
2	0.0489	1.5615e-05	0.0329	
3	1.5615e-05	1.5615e-05	0.0250	
4	0.0172	1.5615e-05	0.0058	
5	1.5615e-05	1.5615e-05	0.0261	
6	1.5615e-05	1.5615e-05	0.0073	
7	1.5615e-05	1.5615e-05	0.0097	
8	1.5615e-05	1.5615e-05	0.0201	
9	1.5615e-05	1.5615e-05	0.0124	
10	1.5615e-05	0.0058	8.2963e-04	
11	1.5615e-05	0.0138	0.0067	
12	1.5615e-05	1.5615e-05	0.0073	

Figure 15: Three component training data

8.2 CLASSIFIED IMAGES

The obtained models were then used to classify the entire sampled image.

- Image pixels of class:settlement were assigned red colour.
- Image pixels of class:vegetation were assigned green colour.
- Image pixels of class:water were assigned blue colour.

The final images obtained from the code are as shown below.

USING DECISION TREE CLASSIFIER

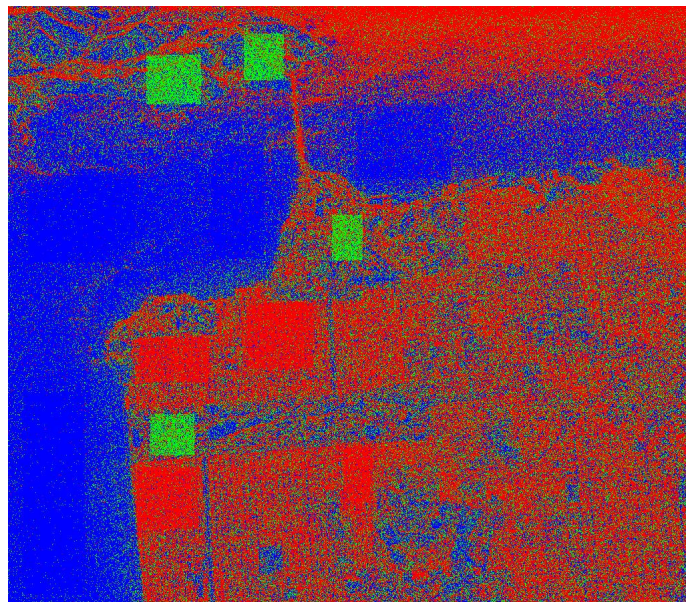


Figure 16: Decision tree classifier image:using three component data

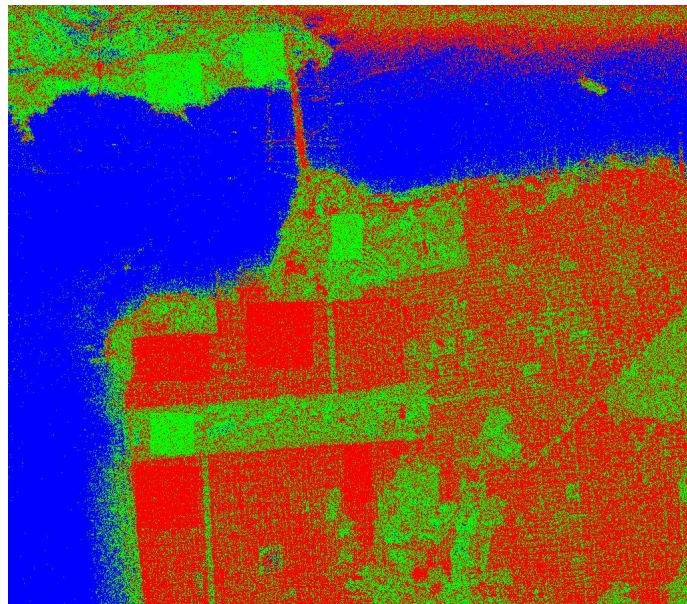


Figure 17: Decision tree classifier image:using four component data

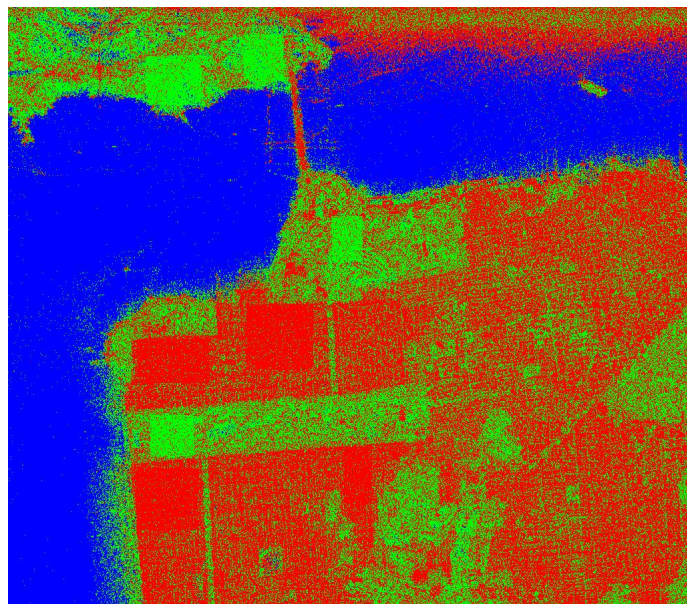


Figure 18: Decision tree classifier image:using seven component data

USING RANDOM FOREST CLASSIFIER

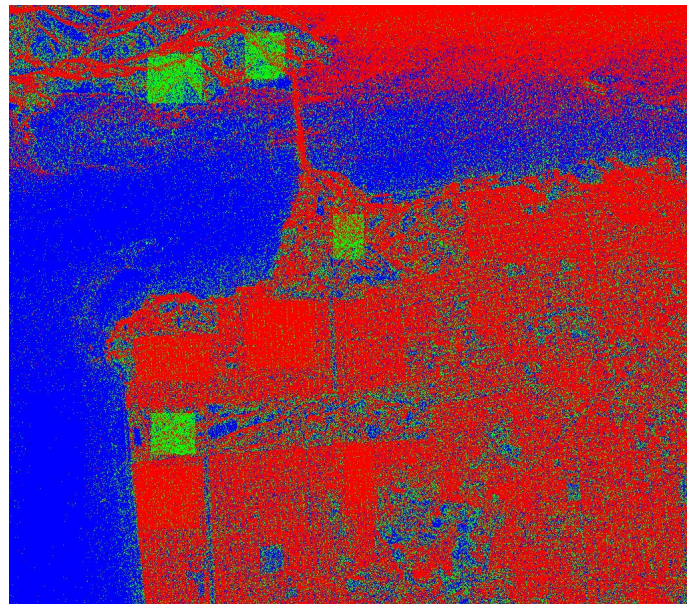


Figure 19: Random Forest classifier image:using three component data

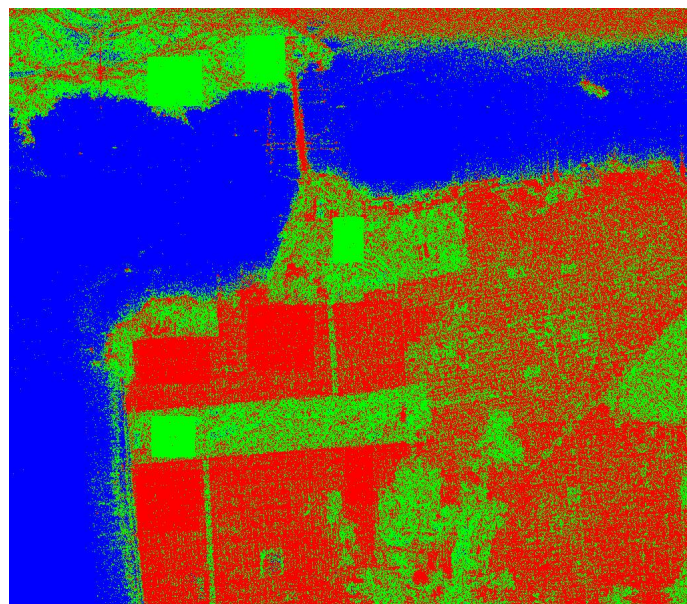


Figure 20: Random Forest classifier image:using four component data

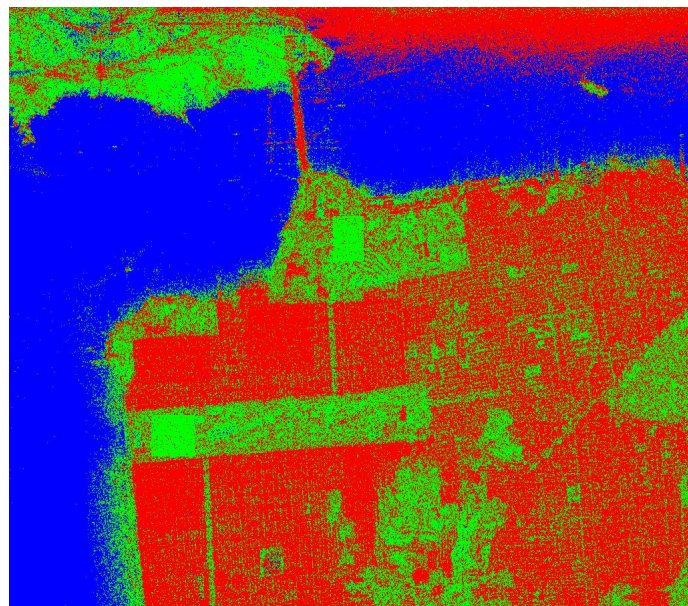


Figure 21: Random Forest classifier image:using seven component data

USING ARTIFICIAL NEURAL NETWORK CLASSIFIER

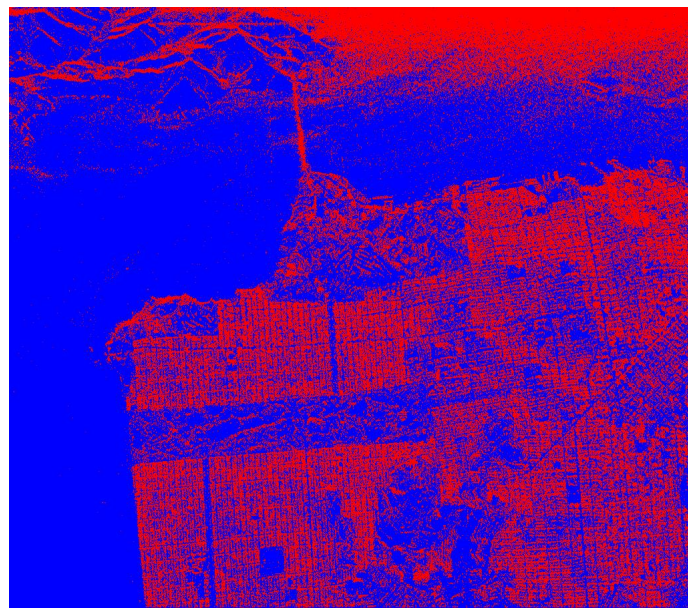


Figure 22: ANN classifier image:using three component data

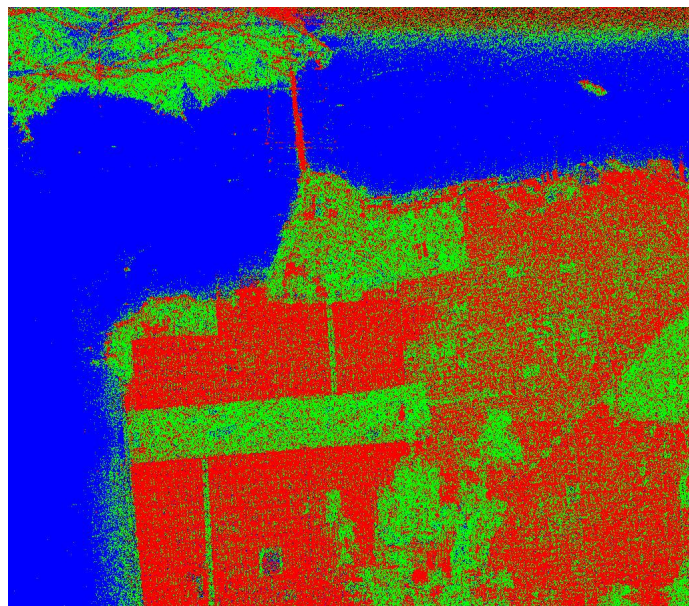


Figure 23: ANN classifier image:using four component data

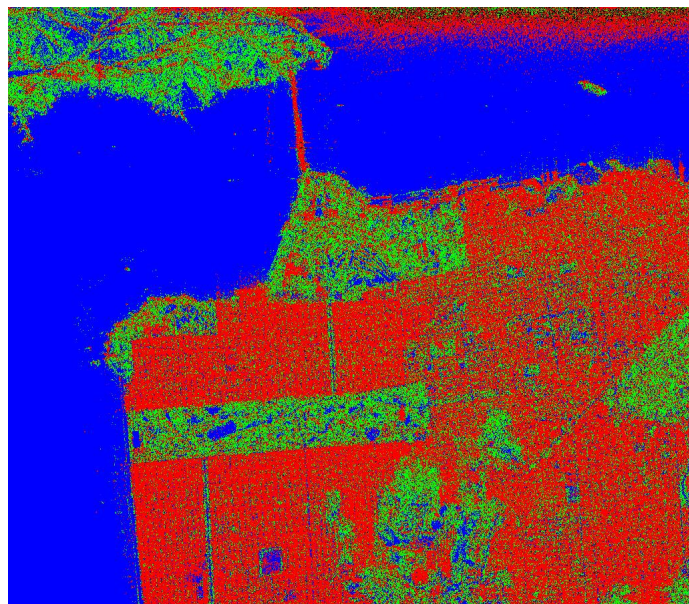


Figure 24: ANN classifier image:using seven component data

8.3 CONFUSION MATRIX

A confusion matrix is a table that is often used to describe the performance of a classification model (or “classifier”) on a set of test data for which the true values are known.

- It allows the visualization of the performance of an algorithm.
- It allows easy identification of confusion between classes e.g. one class is commonly mis-labeled as the other.
- The number of correct and incorrect predictions are summarized with count values and broken down by each class.

Confusion matrices obtained for the 9 test models obtained are explained below, training areas were as follows

Class 1 : Settlement areas

Class 2 : Vegetation areas

Class 3 : Water Body areas

8.3.1 MATRICES FOR DECISION TREE CLASSIFIER MODEL

		PREDICTED CLASS		
		Settlements	Vegetation	Water Bodies
TRUE CLASS	Settlements	84.84%	08.80%	06.36%
	Vegetation	14.00%	76.44%	09.56%
	Water Bodies	05.32%	05.10%	89.58%

Figure 25: Confusion matrix:Decision tree classifier model trained using 3 component data

- 84.84% of the Settlement samples were correctly classified while 8.80% were reclassified as Vegetation and 6.36% of the samples were reclassified as Water bodies.
- 76.44% of the samples of Vegetation class were correctly classified while 14% of the samples were reclassified as Settlements and 9.56% were reclassified as Water bodies.
- 89.58% of the samples of Water Bodies class were correctly classified while 5.32% of the samples were reclassified as Settlements and 5.10% were reclassified as Vegetation.

- Out of 1,76,118 total samples, 1,49,731 samples were correctly classified while the rest were reclassified by the classification model.
- This gets the above classification model to an overall classification accuracy of 85.01%

		PREDICTED CLASS		
		Settlements	Vegetation	Water Bodies
T R U E C L A S S	Settlements	93.51%	06.34%	00.13%
	Vegetation	08.45%	90.50%	01.05%
	Water Bodies	00.23%	00.57%	99.20%

Figure 26: Confusion matrix:Decision tree classifier model trained using 4 component data

- 93.51% of the Settlement samples were correctly classified while 6.34% were reclassified as Vegetation and 0.13% of the samples were reclassified as Water bodies.
- 90.50% of the samples of Vegetation class were correctly classified while 8.45% of the samples were reclassified as Settlements and 1.05% were reclassified as Water bodies.
- 99.20% of the samples of Water Bodies class were correctly classified while 0.23% of the samples were reclassified as Settlements and 0.57% were reclassified as Vegetation.
- Out of 1,76,118 total samples, 1,68,046 samples were correctly classified while the rest were reclassified by the classification model.
- This gets the above classification model to an overall classification accuracy of 95.41%

		PREDICTED CLASS		
		Settlements	Vegetation	Water Bodies
TRUE CLASS	Settlements	93.43%	06.27%	00.30%
	Vegetation	08.08%	90.28%	01.64%
	Water Bodies	00.22%	00.69%	99.09%

Figure 27: Confusion matrix:Decision tree classifier model trained using 7 component data

- 93.43% of the Settlement samples were correctly classified while 6.27% were reclassified as Vegetation and 0.30% of the samples were reclassified as Water bodies.
- 90.28% of the samples of Vegetation class were correctly classified while 8.08% of the samples were reclassified as Settlements and 1.64% were reclassified as Water bodies.
- 99.09% of the samples of Water Bodies class were correctly classified while 0.22% of the samples were reclassified as Settlements and 0.69% were reclassified as Vegetation.
- Out of 1,76,118 total samples, 1,67,827 samples were correctly classified while the rest were reclassified by the classification model.
- This gets the above classification model to an overall classification accuracy of 95.29%

8.3.2 MATRICES FOR ARTIFICIAL NEURAL NETWORK CLASSIFIER MODEL

		PREDICTED CLASS		
		Settlements	Vegetation	Water Bodies
TRUE CLASS	Settlements	41.12%	00.00%	58.88%
	Vegetation	15.18%	00.02%	84.80%
	Water Bodies	02.94%	00.00%	97.05%

Figure 28: Confusion matrix:ANN classifier model trained using 3 component data

- 41.12% of the Settlement samples were correctly classified while 0.00% was reclassified as Vegetation and 58.88% of the samples were reclassified as Water bodies.
- 0.02% of the samples of Vegetation class were correctly classified while 15.18% of the samples were reclassified as Settlements and 84.80% were reclassified as Water bodies.
- 97.05% of the samples of Water Bodies class were correctly classified while 2.94% of the samples were reclassified as Settlements and 0.00% was reclassified as Vegetation.
- Out of 1,76,118 total samples, 1,00,602 samples were correctly classified while the rest were reclassified by the classification model.
- This gets the above classification model to an overall classification accuracy of 57.12%

		PREDICTED CLASS		
		Settlements	Vegetation	Water Bodies
TRUE CLASS	Settlements	79.51%	17.33%	03.14%
	Vegetation	20.90%	67.51%	11.58%
	Water Bodies	00.16%	00.55%	99.27%

Figure 29: Confusion matrix: ANN classifier model trained using 4 component data

- 79.51% of the Settlement samples were correctly classified while 17.33% was reclassified as Vegetation and 3.14% of the samples were reclassified as Water bodies.
- 67.51% of the samples of Vegetation class were correctly classified while 20.9% of the samples were reclassified as Settlements and 11.58% were reclassified as Water bodies.
- 99.27% of the samples of Water Bodies class were correctly classified while 0.16% of the samples were reclassified as Settlements and 0.55% was reclassified as Vegetation.
- Out of 1,76,118 total samples, 1,51,066 samples were correctly classified while the rest were reclassified by the classification model.
- This gets the above classification model to an overall classification accuracy of 85.77%

		PREDICTED CLASS		
		Settlements	Vegetation	Water Bodies
TRUE CLASS	Settlements	79.55%	17.65%	02.79%
	Vegetation	20.20%	69.10%	10.68%
	Water Bodies	00.12%	00.81%	99.05%

Figure 30: Confusion matrix: ANN classifier model trained using 7 component data

- 79.55% of the Settlement samples were correctly classified while 17.65% was reclassified as Vegetation and 2.79% of the samples were reclassified as Water bodies.
- 69.10% of the samples of Vegetation class were correctly classified while 20.2% of the samples were reclassified as Settlements and 10.68% were reclassified as Water bodies.
- 99.05% of the samples of Water Bodies class were correctly classified while 0.12% of the samples were reclassified as Settlements and 0.81% was reclassified as Vegetation.
- Out of 1,76,118 total samples, 1,51,583 samples were correctly classified while the rest were reclassified by the classification model.
- This gets the above classification model to an overall classification accuracy of 86.06%

8.3.3 MATRICES FOR RANDOM FOREST CLASSIFIER MODEL

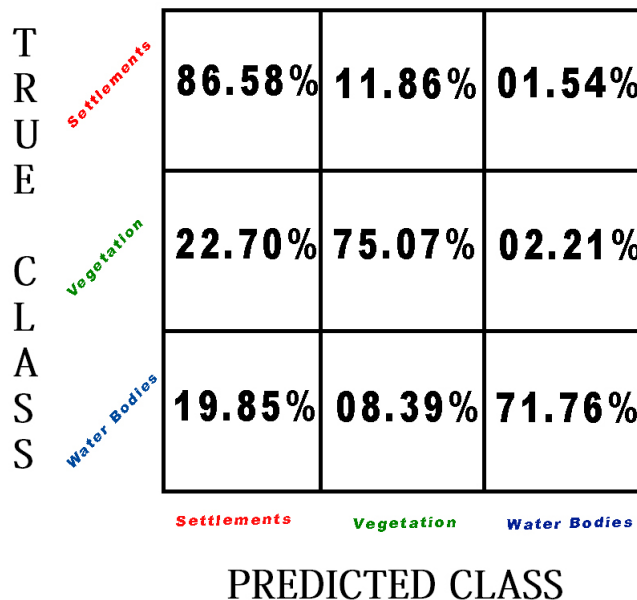


Figure 31: Confusion matrix:Random Forest classifier model trained using 3 component data

- 86.58% of the Settlement samples were correctly classified while 11.86% was reclassified as Vegetation and 1.54% of the samples were reclassified as Water bodies.
- 75.07% of the samples of Vegetation class were correctly classified while 22.7% of the samples were reclassified as Settlements and 2.21% were reclassified as Water bodies.
- 71.76% of the samples of Water Bodies class were correctly classified while 19.85% of the samples were reclassified as Settlements and 8.39% was reclassified as Vegetation.
- Out of 1,76,118 total samples, 1,46,616 samples were correctly classified while the rest were reclassified by the classification model.
- This gets the above classification model to an overall classification accuracy of 83.24%

		PREDICTED CLASS		
		Settlements	Vegetation	Water Bodies
TRUE CLASS	Settlements	97.50%	02.48%	00.01%
	Vegetation	00.68%	99.14%	00.16%
	Water Bodies	00.01%	00.04%	99.95%

Figure 32: Confusion matrix:Random Forest classifier model trained using 4 component data

- 97.5% of the Settlement samples were correctly classified while 2.48% was reclassified as Vegetation and 0.01% of the samples were reclassified as Water bodies.
- 99.14% of the samples of Vegetation class were correctly classified while 0.68% of the samples were reclassified as Settlements and 0.16% were reclassified as Water bodies.
- 99.95% of the samples of Water Bodies class were correctly classified while 0.01% of the samples were reclassified as Settlements and 0.04% was reclassified as Vegetation.
- Out of 1,76,118 total samples, 174408 samples were correctly classified while the rest were reclassified by the classification model.
- This gets the above classification model to an overall classification accuracy of 99.02%

		PREDICTED CLASS		
		Settlements	Vegetation	Water Bodies
TRUE CLASS	Settlements	90.70%	08.04%	01.26%
	Vegetation	02.15%	93.61%	04.23%
	Water Bodies	00.04%	00.52%	99.42%

Figure 33: Confusion matrix:Random Forest classifier model trained using 7 component data

- 99.7% of the Settlement samples were correctly classified while 8.04% was reclassified as Vegetation and 1.26% of the samples were reclassified as Water bodies.
- 93.61% of the samples of Vegetation class were correctly classified while 2.15% of the samples were reclassified as Settlements and 4.23% were reclassified as Water bodies.
- 99.42% of the samples of Water Bodies class were correctly classified while 0.04% of the samples were reclassified as Settlements and 0.52% was reclassified as Vegetation.
- Out of 1,76,118 total samples, 168079 samples were correctly classified while the rest were reclassified by the classification model.
- This gets the above classification model to an overall classification accuracy of 95.43%

8.3.4 PARAMETERS CALCULATED

The following terms are calculated by making use of the data available.

- Producers Accuracy:It is the number of reference sites classified accurately divided by the total number of reference sites for that class.

$$ProdAcc = (correctlyClassified)/(totalSites)$$

- Users Accuracy:The User's Accuracy is calculated by taking the total number of correct classifications for a particular class and dividing it by the row total.

$$UsersAcc = (No.ofClass)/(RowTotal)$$

- Error-Rate:- Error rate (ERR) is calculated as the number of all incorrect predictions divided by the total number of the dataset. The best error rate is 0.0, whereas the worst is 1.0.
- Total Accuracy:-Accuracy (ACC) is calculated as the number of all correct predictions divided by the total number of the dataset. The best accuracy is 1.0, whereas the worst is 0.0. It can also be calculated by $1 - \text{ERR}$.

$$\text{TotalAcc} = (TP + TN) / (TP + TN + FP + FN)$$

- Random Accuracy:-Random Accuracy is defined as the sum of the products of reference likelihood and result likelihood for each class.

$$\text{RandAcc} = ((\text{ActFalse} * \text{PredFalse}) + (\text{ActTrue} * \text{PredTrue})) / \text{total} * \text{total}$$

- Sensitivity:-Sensitivity (SN) is calculated as the number of correct positive predictions divided by the total number of positives. It is also called recall (REC) or true positive rate (TPR).

$$\text{Sensitivity(Recall)} = TP / (TP + FN)$$

- Specificity(True negative Rate):-Specificity (SP) is calculated as the number of correct negative predictions divided by the total number of negatives. It is also called true negative rate (TNR).
- Precision(Positive Predictive value):-Precision (PREC) is calculated as the number of correct positive predictions divided by the total number of positive predictions. It is also called positive predictive value (PPV).

$$\text{Precision} = TP / (TP + FP)$$

- False Positive Rate:-False positive rate (FPR) is calculated as the number of incorrect positive predictions divided by the total number of negatives. The best false positive rate is 0.0 whereas the worst is 1.0.
- Kappa Statistic:-The Kappa Coefficient is generated from a statistical test to evaluate the accuracy of a classification. Kappa essentially evaluates how well the classification is performed as compared to just randomly assigning values, i.e. it checks if the classification did better than the random assignment.

$$\kappa = (\text{TotalAcc} - \text{RandomAcc}) / (1 - \text{RandomAcc})$$

9 COST ANALYSIS

For the purpose of obtaining a rough estimate of the project cost the basic Constructive Cost Model (CoCoMo) was used. The project was categorized as an Organic project.

In order to obtain the final cost the present attribute values at the time of writing this report were taken of the internet. The formulae coefficients corresponding to the project mode selected were assumed.

9.0.1 CHARACTERISTIC CALCULATIONS

Effort

$$Effort = A * (KLOC)^B pm = 0.896 * (1.33)^{1.05} = 1.20879pm$$

Development Time

$$Tdev = C * (Effort)^D Months = 2.5 * (1.2088)^{0.38} = 2.68679months$$

Professionals Required

$$Effort/Tdev = 1.2088/2.686 = 0.450$$

9.0.2 COST ESTIMATION

Technical work cost

Average computer programmer salary per month = ₹ 40,713

Time taken to develop the product = 2.7 months

Cost of hiring a programmer to develop the product = ₹ 1,09,925

Cost of Hardware purchased

HP OMEN 870-244 Desktop Computer: ₹ 1,12,482

Cost of Software purchased

MATLAB licence cost : ₹ 11250

Office space

cost of 3 months at a coworking space: ₹ 30000

Other

Miscellaneous expenses: ₹ 10000

Total Cost

Total Cost was estimated up to: ₹ 2,73,657

10 CONCLUSION

In order to classify the dataset into different classes nine different classification models were used

- The first model used a binary tree classifier which was trained using a 3 component dataset shown in [fig:14]
- The second model used a binary tree classifier which was trained using a 4 component dataset shown in [fig:13]
- The third model used a binary tree classifier which was trained using a 7 component dataset shown in [fig:12]
- The fourth model used an Artificial Neural Network classifier which was trained using a 3 component dataset shown in [fig:14]
- The fifth model used an Artificial Neural Network classifier which was trained using a 4 component dataset shown in [fig:13]
- The sixth model used an Artificial Neural Network classifier which was trained using a 7 component dataset shown in [fig:12]
- The seventh model used a Random Forest classifier which was trained using a 3 component dataset shown in [fig:14]
- The eighth model used a Random Forest classifier which was trained using a 4 component dataset shown in [fig:13]
- The ninth model used a Random Forest classifier which was trained using a 7 component dataset shown in [fig:12]

Based on visual interpretation and observations made from the confusion matrices the following conclusions could be made:

- Of the three datasets used in the project Yamaguchi's four component dataset was found to be the best training dataset since it provided the most accurate results
- Out of the three classifier models used the Random forest classifier was found to provide the most accurate results when compared to the binary tree classifier and ANN classifier
- A combination of the Random Forest classifier trained using Yamaguchi's four component dataset [fig:12] was found to provide the most accurate and acceptable result as shown in [Fig:20]

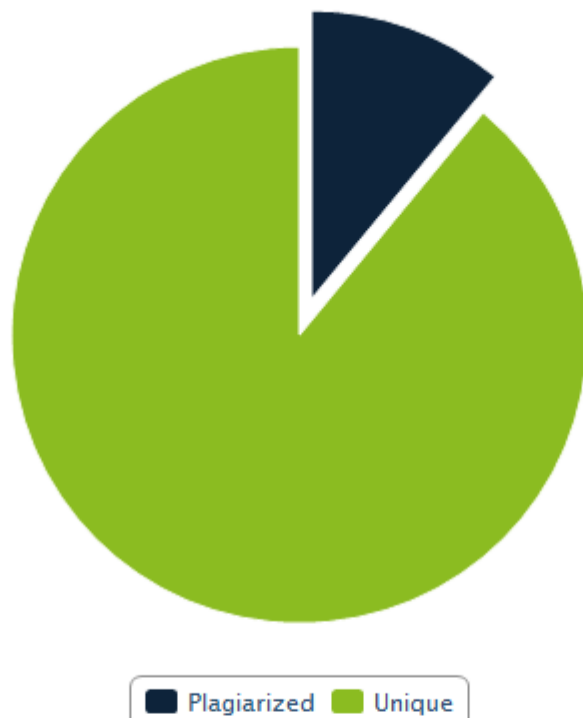
11 BIBLIOGRAPHY

References

- [1] Boussad Azmedroub, Mounira Ouarzeddine, and Boularbah Souissi. Extraction of urban areas from polarimetric sar imagery. *IEEE Journal of Selected Topics in Applied Earth Observations and Remote Sensing*, 9(6):2583–2591, 2016.
- [2] Canada Centre for Remote Sensing. *Fundamentals of Remote sensing*. Canada Centre for Remote Sensing, 2003.
- [3] Ronny Hänsch and Olaf Hellwich. Random forests for building detection in polarimetric sar data. In *2010 IEEE International Geoscience and Remote Sensing Symposium*, pages 460–463. IEEE, 2010.
- [4] Hongying Liu, Dexiang Zhu, Shuyuan Yang, Biao Hou, Shuiping Gou, Tao Xiong, and Licheng Jiao. Semisupervised feature extraction with neighborhood constraints for polarimetric sar classification. *IEEE Journal of Selected Topics in Applied Earth Observations and Remote Sensing*, 9(7):3001–3015, 2016.
- [5] Toshifumi Moriyama, Seiho Uratsuka, Toshihiko Umehara, Makoto Satake, Akitsugu Nadai, Hideo Maeno, Kazuki Nakamura, and Yoshio Yamaguchi. A study on extraction of urban areas from polarimetric synthetic aperture radar image. In *IGARSS 2004. 2004 IEEE International Geoscience and Remote Sensing Symposium*, volume 1. IEEE, 2004.
- [6] YS Rao and Varsha Turkar. Classification of polarimetric sar data over wet and arid regions of india. In *2009 IEEE International Geoscience and Remote Sensing Symposium*, volume 3, pages III–892. IEEE, 2009.
- [7] Maryam Salehi, Mahmod Reza Sahebi, and Yasser Maghsoudi. Improving the accuracy of urban land cover classification using radarsat-2 polsar data. *IEEE Journal of selected topics in applied Earth Observations and Remote Sensing*, 7(4):1394–1401, 2013.
- [8] Gulab Singh, Rashmi Malik, Shradha Mohanty, Virendra Singh Rathore, Kanta Yamada, Maito Umemura, and Yoshio Yamaguchi. Seven-component scattering power decomposition of polsar coherency matrix. *IEEE Transactions on Geoscience and Remote Sensing*, 57(11):8371–8382, 2019.
- [9] Gulab Singh, Shradha Mohanty, Yoshihiro Yamazaki, and Yoshio Yamaguchi. Physical scattering interpretation of polsar coherency matrix by using compound scattering phenomenon. *IEEE Transactions on Geoscience and Remote Sensing*, 2019.
- [10] Varsha Turkar, Rinki Deo, YS Rao, Shiv Mohan, and Anup Das. Classification accuracy of multi-frequency and multi-polarization sar images for various land covers. *IEEE Journal of Selected Topics in Applied Earth Observations and Remote Sensing*, 5(3):936–941, 2012.
- [11] Yoshio Yamaguchi, Yuki Yajima, and Hiroyoshi Yamada. A four-component decomposition of polsar images based on the coherency matrix. *IEEE Geoscience and Remote Sensing Letters*, 3(3):292–296, 2006.

12 PLAGIARISM CHECK RESULT

PlagiarismCheckerX Summary Report



Date	Friday, May 29, 2020
Words	818 Plagiarized Words / Total 7176 Words
Sources	More than 90 Sources Identified.
Remarks	Low Plagiarism Detected – Your Document needs Optional Improvement.

Figure 34: Plagiarism check result